



[www.ericjournal.ait.ac.th](http://www.ericjournal.ait.ac.th)

## ANN Based Modeling of Performance and Emission Characteristics of Diesel Engine Fuelled with Polanga Biodiesel at Different Injection Pressures

Abhishek Sharma\*<sup>1</sup>, Harshdeep Sharma<sup>+</sup>, P.K. Sahoo<sup>#</sup>, R.K. Tripathi<sup>#</sup>, L.C. Meher<sup>&</sup>

**Abstract** – The present work predicts the performance and exhaust parameters of a single cylinder 4-stroke diesel engine at different injection pressures using blended mixture of Polanga biodiesel and diesel by artificial neural network (ANN). Experimental data for training and testing in the proposed ANN was obtained at a constant speed and full load condition. An ANN model was developed based on standard Back- Propagation algorithm for the engine. Multi layer perception network (MLP) was used for non-linear mapping between the input and output parameters. Different activation functions and several rules were used to assess the percentage error between the desired and the predicted values. It was observed that the ANN model can predict the engine performance and exhaust emissions quite well with correlation coefficient (R) 0.99998, 0.9999, 0.99998, 0.9999, 0.9958, 0.9993, 0.9999 for the brake specific fuel consumption, brake thermal efficiency, exhaust gas temperature, NO<sub>x</sub>, CO, smoke and UBHC emissions, respectively.

**Keywords** – Artificial neural network, biodiesel, diesel engine, emission and performance.

### 1. INTRODUCTION

Rapidly increasing energy demand due to industrialization has led to a large number of developing countries importing crude oil. Thus, a major part of their export earnings is spent on purchase of petroleum products. The other problem of concern is the degradation of environment due to fossil fuel combustion besides the fuel crisis. Thus it is essential that low emission alternate fuels must be developed for use in diesel engines. Biodiesel has been widely recognized in the alternative fuel industry due its attractive features: (i) it is plant-derived, and as such its combustion does not increase current net atmospheric levels of greenhouse gas (ii) it can be domestically produced, offering the possibility of reducing petroleum imports; (iii) it is biodegradable; and (iv) relative to conventional diesel fuel, its combustion products have reduced levels of particulates, carbon monoxide, and, in some conditions, nitrogen oxides [1]. The research and development activities on biodiesel have been mostly on sunflowers, saffola, soyabean, rapeseed and peanut which are considered edible in several countries [2]-[3]. However, biodiesel can also be produced from non-edible oil seeds like jatropha, karanja, neem, cotton, rubber and polanga, etc. [4]. Sahoo *et al.* [2], conducted engine tests using Polanga based biodiesel and recommended its use as an alternative fuel for the existing conventional diesel engines without any major hardware modifications. The density and viscosity of the Polanga oil methyl ester formed after triple stage

transesterification were found to be close to those of petroleum diesel oil. Sahoo *et al.* [5] evaluated comparative performance and emission characteristics of jatropha, karanja and polanga based biodiesel as fuel in a tractor engine. They observed that brake specific fuel consumption for all the biodiesel blends with diesel increased with blends and decreased with speed. The study however lacks the effect of injection pressure on engine performance. Injection pressure along with blend percentage is also an important parameter that may affect the performance and emission characteristics [6].

The performance of a CI engine for various proportions of blends, for various compression ratios and at different injection timings and pressures are usually desired by engine manufacturers and engineers. This can be obtained either by conducting comprehensive tests or by modeling the engine operation. Testing the engine under all possible operating conditions and fuel cases are both time consuming and expensive. On the other hand developing an accurate model for the operation of a CI engine fuelled with blends of biodiesel is too difficult due to the complex nature of the processes involved. So, as an alternative, engine performance and exhaust emissions can be modeled using Artificial Neural Networks (ANNs). The predictive ability of an ANN results from the training on experimental data and then validation by independent data. An ANN model can accommodate multiple input variables to predict multiple output variables. The prediction by a well-trained ANN is normally much faster than the conventional simulation programs or mathematical models as no lengthy iterative calculations are needed to solve differential equations using numerical methods but the selection of an appropriate neural network topology is important in terms of model accuracy and model simplicity. In addition, it is possible to add or remove input and output variables in the ANN if it is needed. Canakci *et al.* [7] investigated the engine performance and emissions characteristics of two different petroleum diesel-fuels

\*Ideal Institute of Technology, Ghaziabad, 201002, India.

<sup>+</sup>School of Mechanical Engineering., Galgotias University, G. Noida, India.

<sup>#</sup> College of Engineering Studies, UPES, Dehradun, India.

<sup>&</sup>DRDO, Secundrabad, India.

<sup>1</sup>Corresponding author: Tel: +919711259730.  
E-mail: [absk2001@gmail.com](mailto:absk2001@gmail.com).

(No. 1 and No. 2), biodiesels (from soybean oil and yellow grease) using Artificial Neural Networks where 20% blends with No. 2 diesel fuel were used as experimental results. In this study, the average molecular weight, net heat of combustion, specific gravity, kinematic viscosity, C/H ratio and cetane number of each fuel were used as the input layer, while outputs were the brake specific fuel-consumption, exhaust temperature, and exhaust emissions. The back-propagation learning algorithm with three different variants, single layer, and logistic sigmoid transfer function were used in the network. The network yielded  $R^2$  values of 0.99 for both training and test data. The mean % errors were smaller than 4.2 and 5.5 for the training and test data respectively. Ghobadian *et al.* [1] developed an artificial neural network model of a diesel engine using waste cooking biodiesel fuel with standard Back-Propagation algorithm. The developed model predicted the engine performance and exhaust emissions quite well with correlation coefficient (R) 0.9487, 0.999, 0.929 and 0.999 for the engine torque, SFC, CO and HC emissions, respectively. The predicted MSE (Mean Square Error) was between the desired outputs as measured values and the simulated values were obtained as 0.0004 by the model. Canakci *et al.* [8] used ANN to model performance parameters and emissions of a biodiesel engine using waste cooking oil. Engine speed and percentage of blend were taken as the input variables and brake power, torque, specific fuel consumption and exhaust emissions as the outputs. It was observed that the regression values for most of the parameters were close to unity. Yusaf *et al.* [9] conducted experiments in a diesel engine fuelled with a combination of both compressed natural gas and diesel fuel. ANN modeling was used to predict brake power, torque, brake specific fuel consumption and engine emissions. A good correlation between predicted and the experimental values was observed. Ismail *et al.* [10] reported an artificial neural network model programmed for a light-duty diesel engine. Engine operating parameters viz., engine speed, output torque, fuel mass flow rate and biodiesel fuel types and blends, were used as the input parameters in the model. The results indicated that back-propagation feed-forward neural network, combination of tansig/purelin transfer functions, trainlm training algorithm were the optimum configuration to predict the correlations. Çay *et al.* [11] used artificial neural network (ANN) modeling to predict the brake specific fuel consumption, effective power and average effective pressure and exhaust gas temperature of the methanol engine. It was found that the  $R^2$  values were close to 1 for both training and testing data. RMS values were smaller than 0.015 and mean errors were smaller than 3.8% for the testing data. Wong *et al.* [12] evaluated optimal biodiesel ratio that could achieve the goals of fewer emissions, reasonable fuel economy and wide engine operating range. Different advanced machine learning techniques, namely ELM (extreme learning machine), LS-SVM (least-squares support vector machine) and RBFNN (radial-basis function neural network), were used to create engine models based on experimental data. Javed

*et al.* [13] investigated the use of ANN modeling for prediction of performance and emission characteristics of a four stroke single cylinder diesel engine with Jatropha Methyl Ester biodiesel blends along with hydrogen in dual fuel mode. Seven training algorithms each with five combinations of trainings functions were investigated. Levenberg-Marquardt back propagation training algorithm with logarithmic sigmoid and hyperbolic tangent sigmoid transfer function resulted in best model for prediction of performance and emissions characteristics. Wong *et al.* [14] proposed a new biodiesel engine modeling and optimization framework based on extreme learning machine to achieve the goal of fewer emissions, low fuel cost and wide engine operating range. Logarithmic transformation of dependent variables was used to alleviate the problems of data scarcity and data exponentiality simultaneously. With the K-ELM engine model, cuckoo search (CS) was then employed to determine the optimal biodiesel ratio. The evaluation result showed that K-ELM can achieve comparable performance to LS-SVM, resulting in a reliable prediction result for optimization. It also showed that the optimization results based on CS was effective. In the present work, experimental investigations of the performance and emissions of the diesel engine were conducted for different proportions of blends of Polanga with diesel at different injection pressures for full load condition. Using data from experimental results, ANN models have been developed for the performance parameters and emissions characteristics. In the model, blends of Polanga with diesel, different injection pressures are taken as input parameters and brake specific fuel consumption, brake thermal efficiency, exhaust gas temperature, CO, NO<sub>x</sub>, smoke and UBHC emissions are taken as output parameters.

## 2. EXPERIMENTAL INVESTIGATION

The engine used in the present study was a Kirloskar make single cylinder four stroke water cooled CI engine. The detailed specification of the engine is shown in Table 1. The schematic diagram of the experimental set up is shown in Figure 1. The experimental set up consists of engine, dynamometer, load cell and temperature sensors *etc.* Figure 2 shows the photographic view of setup.

Eddy current-dynamometer was used for engine loading. A fuel consumption meter, DP transmitter, Range 0-500 mm wc, was used for measuring the specific fuel consumptions of the engine. A quartz (piezoelectric) Kistler makes transducer was used to determine the engine cylinder combustion gas pressure sensor mounted on the cylinder head. The signals from charging amplifier were fed to the data acquisition system where the engine control module converted the signals into digital data. The in-cylinder pressure data in terms of pressure crank angle history was obtained from the Legion Brothers database. The maximum resolution of the pressure sensor was 1°CA. The cylinder pressure signal was passed through an amplifier to give outputs of 0-10volts for the calibrated pressure range of 0-100 bar. Real time data acquisition was done with the help of

Engine test Express V5.76 which was Labview based software package developed by Legion Brothers. The rated frequency of the data acquisition system was 37 kHz and the sampling time used was 60 seconds. This time duration was selected to ensure that the data is representative. All the signals collected from the test rig needed to be converted from an original analogue form to a digital form. This was achieved by using an Analogue to Digital Converter (ADC) interface between

the transducers and the computer. The CED 1401 power ADC is able to record waveforms data, digital (event) data and marker information. It can also generate waveform and digital outputs simultaneously for realtime, multi-tasking experimental system using its own processor, clocks and memory under the control of the host computer. The Analogue to Digital Converter (ADC) has 8 channels, 500 MHz bandwidth and 4Gs/s sampling rate.

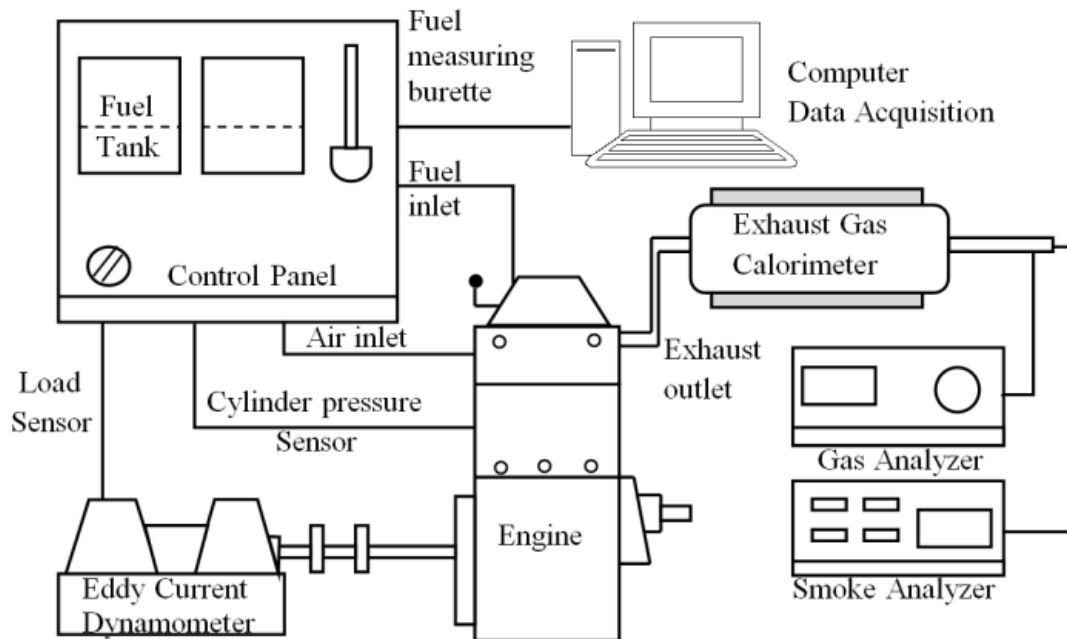
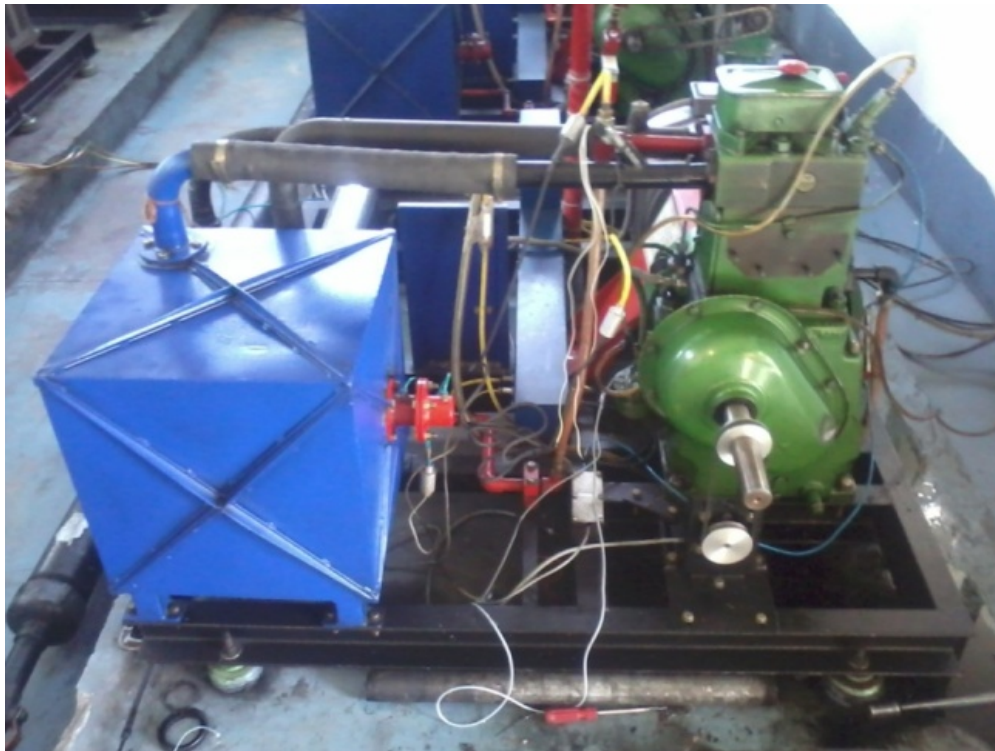


Fig. 1. Experimental setup.

Table 1. Engine specifications.

Item description	KIRLOSKAR
BHP	5HP
Speed	1500
Number of cylinders	1
Compression ration	16.7:1
Bore	80 mm
Stroke	110 mm
Orifice Diameter	20 mm
Type of ignition	Compression ignition
Method of Loading	Eddy current dyanometer
Method of starting	Manual cranking
Method of cooling	Water



**Fig. 2. Photographic view of set up.**

Exhaust gas analyzer of AVL make (AVL DiGas 444) was used for measuring the emissions of HC, CO and NO<sub>x</sub> from the engine. A Smoke meter, model 437C, made by AVL Gurgaon, was used for measuring the smoke emission from engine. Exhaust gas emissions recorded were: unburned hydrocarbons (UBHC) in parts per million (ppm hex), and oxides of nitrogen (NO<sub>x</sub>) in ppm vol. and CO in % vol. by using gas analyzer. Opacity of the smoke in the exhaust was measured in % by using smoke meter. For exhaust gas temperature measurement, Chrome-Alumel K-Type thermocouples with stainless steel wire were implanted close to the engine exhaust manifold. The small micro-voltage outputs from these thermocouples were processed by the Express V5.76 software to give values in degrees centigrade for data logging and engine monitoring purposes. For cooling water temperature measurement, Chrome-Alumel K-Type thermocouples with stainless steel wire were implanted close to the engine water inlet and outlet manifold which gives the temperature of the water also obtained from the Legion Brothers database. The percentage uncertainties of various instruments is given in Table 2.

The performance test of engine included fuel consumption and rating test. In order to carry out fuel

consumption test, initially the engine was started and warmed up on zero loads. After that the engine was gradually loaded up to 100 percent load to stabilize its operation. The experiment with each selected fuel type was replicated three times and the average value of different performance and emission parameters measured was taken for analysis. In the present investigation, biodiesel derived from polanga oil was used as the test fuel. Biodiesel preparation through transesterification process has already been reported in previous studies [2]-[5]. Four biodiesel blends of Polanga were used viz., BD10, BD20, BD30, BD40. The injection pressure of the engine was kept at 180 bars (as set by the manufacturer) and the fuel was altered to biodiesel. The performance, emissions and combustion characteristics of diesel engine were recorded with a constant speed of 1500 rpm. Similar procedures were repeated for other biodiesel blends at the same injection pressure. To visualize the effect of injection pressure, the entire procedure was repeated for injection pressure of 160 bar, 200 bar, 220 bar and 240 bar. The experimental data obtained has been summarized in Table 3.

**Table 2. Percentage uncertainties of various instruments.**

Instruments	Range	Accuracy	Percentage uncertainty
AVL DiGas 444 Gas Analyser			
Hydrocarbon	0-20000 ppm vol	<200: $\pm 10$	$\pm 0.3$
		>200: $\pm 5\%$	
Nitric oxide	0-5000 ppm vol	<500: $\pm 50$	$\pm 0.2$
		>500: $\pm 10\%$	
AVL-437C Smoke meter			
Smoke opacity	0-100%	$\pm 1\%$	$\pm 1$
Exhaust gas temperature	0-1250°C	$\pm 1^\circ\text{C}$	$\pm 0.2$
Burette fuel		$\pm 1\text{cc}$	$\pm 1$
Transducer	0-100 bar	$\pm 0.01\text{bar}$	$\pm 0.1$

**Table 3. Experimental results under different injection pressures and biodiesel blends.**

IP (bar)	BD (%)	BSFC (kg/kWh)	BTE (%)	CO (% vol)	UBHC (ppm)	NO <sub>x</sub> (ppm)
160	10	0.24	38	0.077	41	777
160	20	0.247	36.21	0.07	40	790
160	30	0.258	35.1	0.058	38	826
160	40	0.267	34.02	0.0466	37	866
180	10	0.2268	40.23	0.0712	40	785
180	20	0.24	38.45	0.062	38	800
180	30	0.25	37.25	0.052	36	836
180	40	0.2614	36.66	0.039	35	878
200	10	0.2268	40.6	0.0637	36	797
200	20	0.238	39.31	0.05	34	811
200	30	0.243	38.27	0.043	34	842
200	40	0.2522	37.9	0.0254	31	888
220	10	0.2535	35.77	0.0502	33	807
220	20	0.247	36.63	0.04	32	814
220	30	0.241	37.84	0.029	31	846
220	40	0.2394	38.7	0.019	29	898
240	10	0.262	34.56	0.0366	32	784
240	20	0.2495	37.18	0.027	30	801
240	30	0.238	39.34	0.022	29	835
240	40	0.23	40.18	0.016	28	868



### 3 NEURAL NETWORK DESIGN

#### 3.1 Artificial neural networks

ANNs are logic programming technique developed by imitating the operation of the human brain to perform functions such as learning, remembering, deciding, and inference, without receiving any aid. ANNs have various important features, such as learning from data, generalization, working with an infinite number of variables, etc. Artificial neural cells are the smallest units that form the basis of the operation of ANNs just like a biological neuron which receives inputs from other sources, combines them in some way, performs generally a non-linear operation on the result, and then outputs the final result. The artificial neural cells consist of mainly five elements namely; inputs, weights, summation functions, activation functions and outputs (Figure 3).

ANN has three main layers namely; input, hidden and output layers. The inputs are data from the external source. The processing elements, called neurons, in the input layer transfers data from the external source to the hidden layer. The weights are the values of connections between cells. The outputs are produced using data from neurons in the input and hidden layers, and the bias, summation and activation functions. In the output layer, the output of network is produced by processing data from hidden layer and sent to external source. The summation function is a function which calculates the net input of the cell. The summation function used in this study is given in Equation (1).

$$NT_i = \sum_{j=1}^n w_{ij}x_j + w_{bi} \quad (1)$$

The activation function provides a curvilinear relation between the input and output layers. It also determines the output of the cell by processing the net input to the cell. The selection of an appropriate

activation function significantly affects network performance. Commonly used activation functions are the threshold function, step activation function, sigmoid function, and hyperbolic tangent function. The type of activation function depends on the type of neural network to be designed. A sigmoid function is widely used for the transfer function. Logistic transfer function of the ANN model in this study is given in Equation (2).

$$f(NT_i) = \frac{1}{1 + e^{-NT_i}} \quad (2)$$

The significant advantages of artificial neural networks are learning ability and the use of different learning algorithms. The most important factor which determines its success in practice, after the selection of ANN architecture, is the learning algorithm. In order to obtain the output values closest to the numerical values, the best learning algorithm and the number of optimum neurons in the hidden layer must be determined.

A most sought-after algorithm is the back-propagation algorithm, which has different variants. Back-propagation training algorithms such as conjugate gradient, quasi-Newton, and Levenberg–Marquardt (LM) use standard numerical optimization techniques. ANN with back-propagation algorithm learns by changing the weights which are stored as knowledge. The algorithm uses the second-order derivatives of the cost function so that a better convergence behavior can be obtained. To get the best prediction by the network, several architectures were evaluated and trained using the experimental data. The back-propagation algorithm was utilized in training of all ANN models. In the training stage, to obtain the output precisely, the number of neurons in the hidden layer was increased step by step (*i.e.* 1 to 20). As a result of conducted trials, best learning algorithms for most of the parameters was found to be the Levenberge Marquardt learning algorithm. The best ANN architecture built for prediction of UBHC is shown in Figure 4.

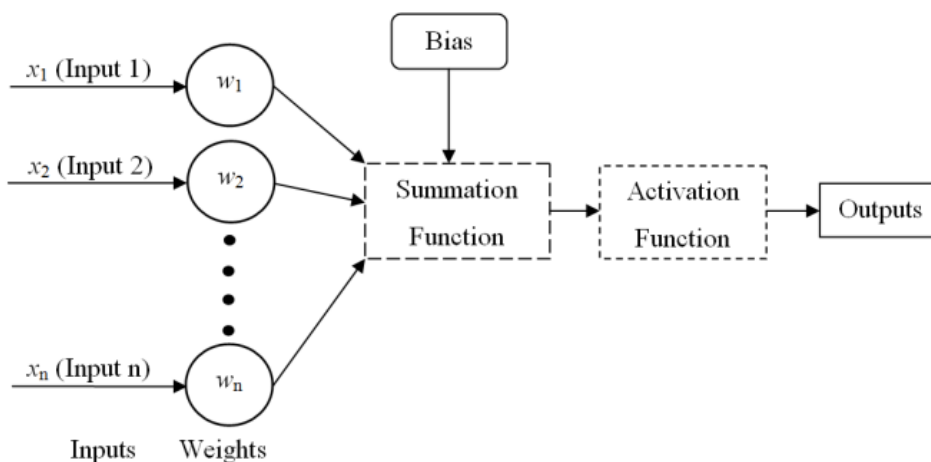


Fig. 3. Structure of an artificial neural cell.

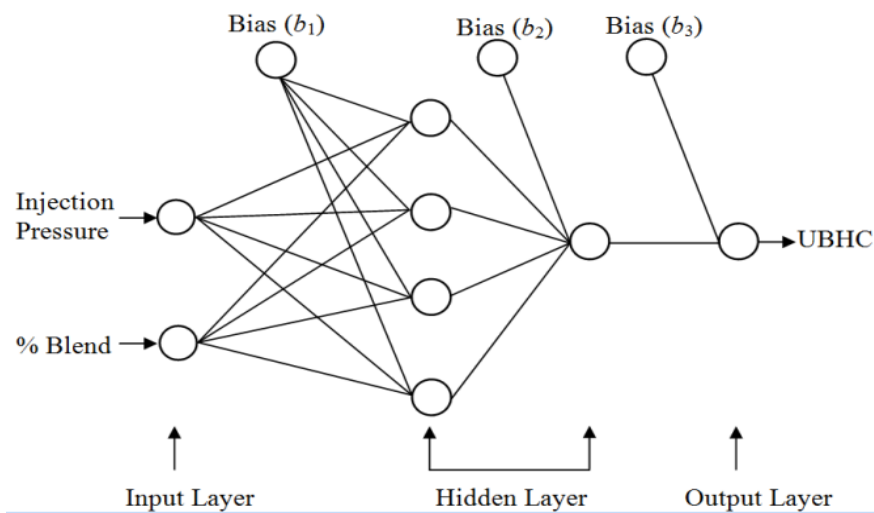


Fig. 4. Best ANN architecture for prediction of UBHC.

Table 4. Correlation coefficients for outputs using different learning algorithms.

Parameter	Activation function	Neurons	Correlation coefficient	
			Training	Testing
BTE	Sig/ lin/lin	3/1	0.9986	0.9617
	Sig/lin/lin	4/1	0.9999	0.9884
	Sig/lin/lin	8/1	0.9999	0.9448
BSFC	Sig/Sig/lin	10/10	0.9998	0.9988
	Sig/lin/lin	5/1	0.9999	0.9959
	Sig/lin/lin	8/1	0.99998	0.99992
Tex	Tan/lin/lin	12/1	0.999	0.996
	Sig/ lin/lin	2/1	0.9968	0.99996
	Sig/lin/lin	4/1	0.9999	0.9982
CO	Sig/lin/lin	6/1	0.99998	0.9996
	Sig/ lin/lin	2/1	0.9941	0.9981
	Sig/lin/lin	4/1	0.9934	0.9998
NO <sub>x</sub>	Sig/lin/lin	6/1	0.99998	0.9958
	Sig/ lin/lin	2/1	0.9951	0.9977
	Sig/lin/lin	4/1	0.9991	0.9984
Smoke	Sig/lin/lin	6/1	0.9999	0.9994
	Sig/ lin/lin	2/1	0.9975	0.9912
	Sig/lin/lin	4/1	0.9993	0.9987
UBHC	Sig/lin/lin	6/1	0.9989	0.9974
	Sig/ lin/lin	2/1	0.9974	0.9983
	Sig/lin/lin	2/1	0.9976	0.9996
	Sig/lin/lin	4/1	0.9999	0.9896

Also, correlation coefficients of BTE, BSFC, Tex, CO, NO<sub>x</sub>, Smoke and UBHC for different learning algorithms are given in Table 4.

In this study, 20 experimental data sets were prepared for the training and testing data for the ANN. The ratio for training and testing data was selected as

70%:30%, i.e. 14 and 6 sets of the experimental data were randomly selected for the data training and testing data, respectively. In the back propagation model, the scaling of inputs and outputs dramatically affects the performance of an ANN. As mentioned above, the logistic sigmoid transfer function was used in this study. One of the characteristics of this function was that only a value between 0 and 1 can be produced. The input and output data sets were normalized between 0.1 and 0.9 before the training and testing process to obtain the optimal predictions. Linear function suited best for the output layer. This arrangement of functions in function approximation problems or modeling is common and yields better results. However many other networks with several functions and topologies were examined. Three criteria were used to evaluate the networks and find the optimum one among them. The training and testing performance (MSE) were chosen to be 0.00001 for all ANNs. The smaller ANNs had the priority to be selected as the complexity and size of the network was also important. Finally, a regression analysis between the network response and the corresponding targets was performed to investigate the network response in more detail. Different training algorithms were also tested and finally Levenberg–Marquardt (Trainlm) was selected. The computer program was developed in MATLAB 2010a. Neural network toolbox was used for ANN design.

## 4. RESULTS AND DISCUSSIONS

### 4.1 Biodiesel fuel characteristics and properties

Biodiesel is produced by the three stage transesterification process. The first stage removes the organic matters and other impurities present in the unrefined filtered polanga oil using reagent. The second stage reduces the acid value of the oil about 4 mg KOH/gm corresponding to a FFA level of 2%. The product of the second stage (pure triglycerides) is transesterified to mono-esters of fatty acids (biodiesel) using alkali catalyst. Fuel properties are mentioned in

Table 5.

### 4.2 Performance Parameters

#### 4.2.1 Brake specific fuel consumption (BSFC)

Table 3 shows BSFC results for different biodiesel-blended diesel fuels and injection pressures at constant load. A decrease in injection pressure increased the BSFC values compared to original injection pressure of 180 bar for all the blends. In this study BSFC results for different biodiesel-blended diesel fuels and injection pressures at constant load. A decrease in injection pressure increased the BSFC values compared to original injection pressure of 180 bar for all the blends due to decreasing injection pressure, fuel particle diameters will enlarge and ignition delay period during the combustion will increase. This situation causes an increase in the BSFC. On the other hand, increasing injection pressure from the original pressure decreases the BSFC values for BD20, BD30 and BD40. The decrease in BSFC can be attributed to the more efficient utilization of the fuel at higher injection pressure because of better atomization associated with slight delay in admission due to high needle lift pressure with same period and hence lesser fuel going to cylinder. For blends BD10 an increase in injection pressure increases the BSFC values due to a shorter ignition delay period. From Figure 5, minimum BSFC for BD10 is 0.226 kg/kW-hr at 180 and 200 bar and increase in injection pressure from 200 to 240 bar, the BSFC is increased to 0.36 kg/kW-hr.

It is found that the BSFC is decreased with increase in injection pressure up to 200 bar. This may be due to that, as injection pressure increases the penetration length and spray cone angle increases. It is also notice that with increasing percentage of polanga biodiesel BSFC decline at elevated injection pressure, from experiments that is find that BD40 shows 0.23 kg/kW-hr fuel consumption at 240 bar injection pressure, that is due to high viscosity of fuel.

**Table 5. Properties of polanga biodiesel and its blends.**

Fuel	CV (KJ/kg)	Viscosity (cSt)	Density (gm/cc)	Flash point (°C)
Diesel	43996.3	2.91	0.830	77
10%B	40094.2	3.1	0.839	82
20%B	39193.7	3.2	0.847	88
30%B	38393.3	3.32	0.855	94
40%B	37792.9	3.6	0.863	99
100%B	36992.5	6.8	0.941	152



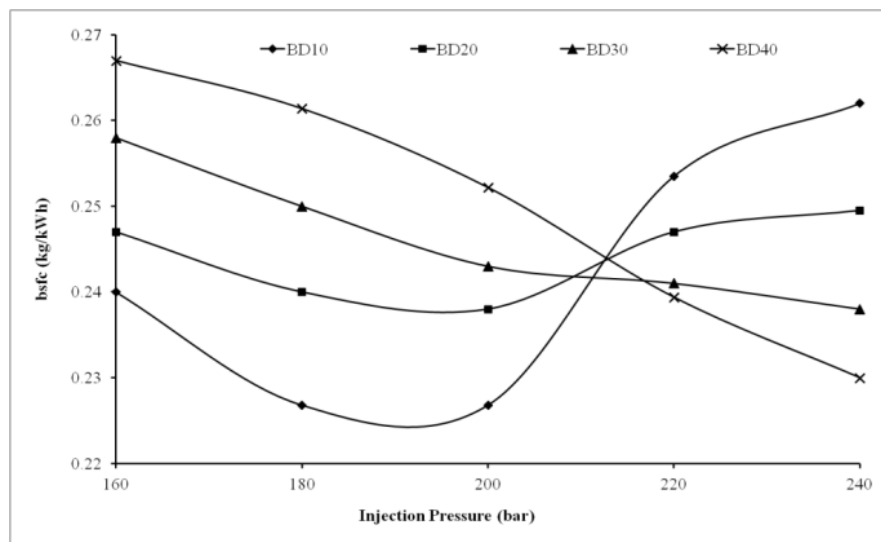


Fig. 5. Variation of BSFC at different injection pressure for different blends.

#### 4.2.2 Brake thermal efficiency (BTE)

The BTE points to the ability of the combustion system to accept the experimental fuel and provides comparable means of assessing how efficient the energy in the fuel was converted to mechanical output. It could be concluded that as the biodiesel amount increases in the fuel blend at the given injection pressure, the BSFC increases, since the Lower calorific value of the blend decreases. BTE is a function of BSFC and Lower calorific value of the blend for a constant effective power. It is clear that Lower calorific value is more effective than BSFC with regard to increasing BTE. The BTE is increased with increase in injection pressure due to the improved atomization and better combustion. The BTE is maximum at 200 bars for BD10 is 40.6% this is due to fine spray formed during injection and improved atomization as shown in Figure 5. Further the BTE tends to decrease, this may be due to that at higher injection pressure the size of fuel droplets decreases and very high fine fuel spray will be injected, because of this, penetration of fuel spray reduces and momentum of fuel droplets will be reduced. Therefore, the BTE generally increased as the biodiesel content increased in the blended fuel for all injection pressures. As demonstrated in Figure 6, the maximum BTE was acquired as 40.18% with the BD40 for 240 bar injection pressure.

#### 4.2.3 Exhaust gas temperature

The variation of exhaust gas temperature with the injection pressure at full load for polanga biodiesel blends is given in Figure 7. In general EGT increases with the load, and for higher injection pressure the exhaust gas temperature is increased since the operating temperature is more at elevated injection pressure. It can be observed that the exhaust gas temperature increases as the percentage of biodiesel is increased. In polanga biodiesel blends operation the combustion is delayed due to higher physical delay period. As the combustion is belated, injected polanga biodiesel fuel particles may not get enough time to burn completely before TDC, hence some fuel mixture tend to burn during the early

part of expansion, consequently after burning occurs and hence increase in the exhaust temperature. The variation with the injection pressure at full load for polanga biodiesel blends is shown in Figure 7.

Table 3 shows  $T_{ex}$  results for different biodiesel-blended diesel fuels and injection pressures at constant load. The exhaust gas temperature is minimum for 160 bar injection pressure for all Polanga blends, minimum 253°C for BD10 polanga blends at 160 bar injection pressure. Increasing the injection pressure increase in exhaust gas temperature ( $T_{ex}$ ) was shown in present study. Maximum exhaust gas temperature ( $T_{ex}$ ) 288°C for BD40 this is due to high oxygen content with at 240 bars injection pressure occur in this study. Of all the blends, BD10 shows lower values of exhaust gas temperature at all the injection pressure, BD40 shows higher values of exhaust gas temperature at all the injection pressure due to increasing oxygen content with increasing blending.

### 4.3 Exhaust emissions

#### 4.3.1 Carbon monoxide

Carbon monoxide results from partial combustion of fuel and it is produced most readily from petroleum fuels, which contain no oxygen in their molecular structure. Usually, CO emissions is affected by air–fuel equivalence ratio, fuel type, combustion chamber design, atomization rate, start of injection timing, injection pressure, engine load and speed. Table 3 shows CO results for different biodiesel-blended diesel fuels and injection pressures at constant load. It is shown from Figure 8 that CO emission level decreased with the increasing biodiesel percentage. This may be due to the more complete combustion of biodiesel with presence of more oxygen in the combustion. From this figure, it was concluded that increased injection pressure narrowed the CO emissions. The increasing injection pressure caused a good fuel–air mixing, easy and complete combustion of the smaller droplets. These effects lead to reduce CO emissions. However, BD 40 shows less emission of CO on all injection pressure. Reduction in CO was observed

with increasing injection pressure for biodiesel. Minimum CO emission of 0.016% by vol. was observed at the injection pressure of 240 bar. This is due to the lower carbon content of biodiesel and also better

combustion caused by the improved atomization, better mixing process at higher injection pressure of 240 bar and maximum CO emission of 0.077% by vol. was observed at the injection pressure of 160 bar for BD10.

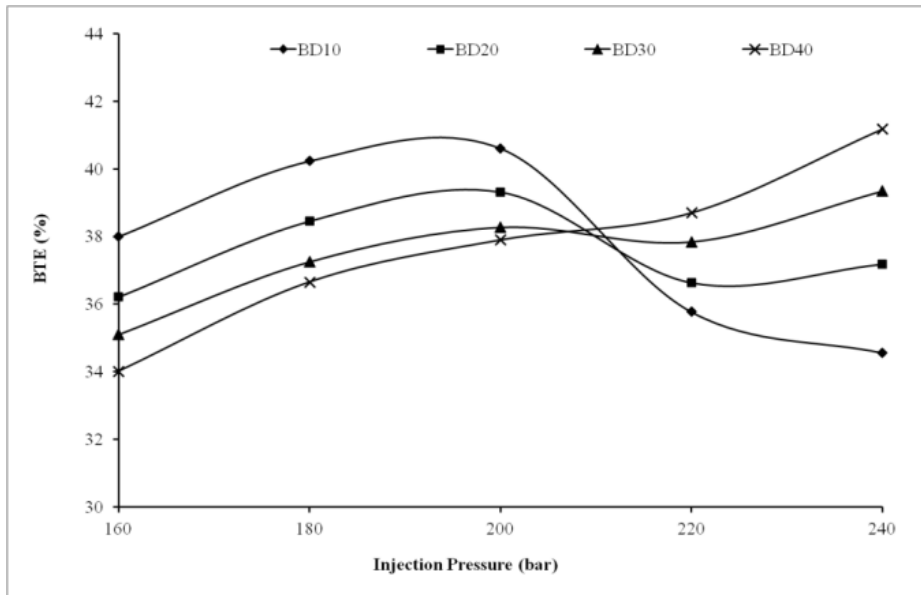


Fig. 6. Variation of BTE with injection pressure

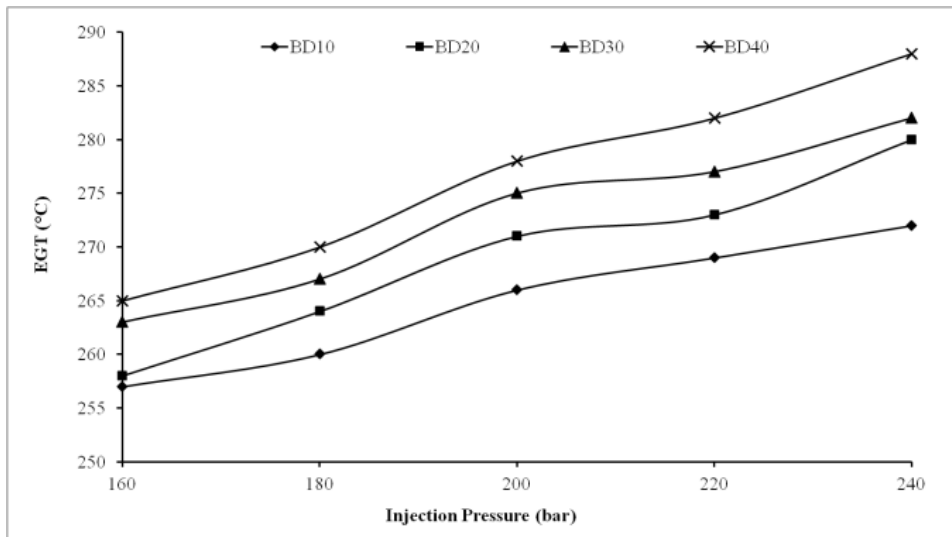


Fig. 7. Variation of exhaust gas temperature ( $T_{ex}$ ) with injection pressure at full load

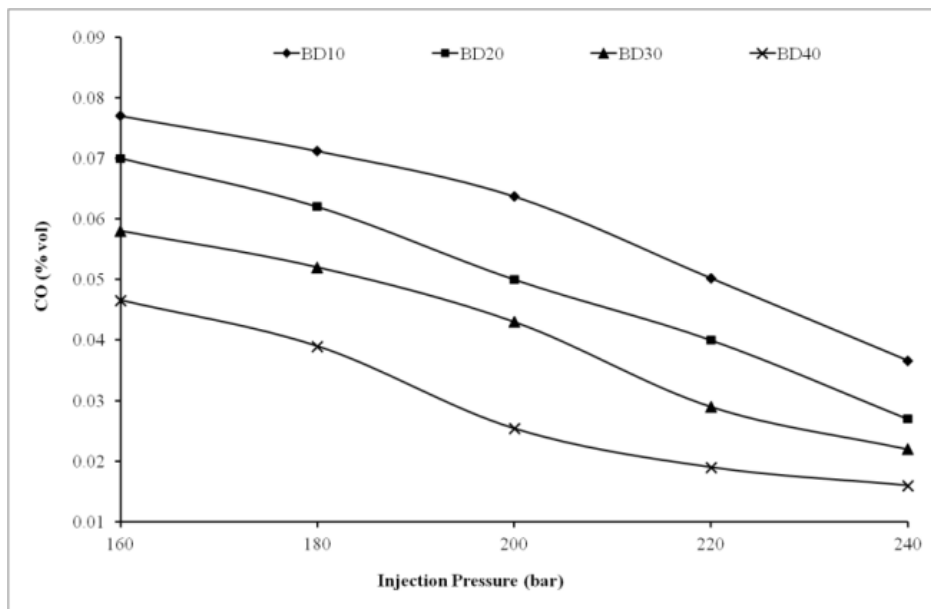


Fig. 8. Emission of carbon monoxide with injection pressure

#### 4.3.2 Un-burnt hydrocarbon emission (UBHC)

Table 3 shows UBHC results for different biodiesel-blended diesel fuels and injection pressures at constant load, un-burnt hydrocarbon emission emissions consist of fuel that is completely unburned or only partially burned. UBHC emissions result from the problems of fuel and air mixing, and largely unaffected by the overall air–fuel equivalence ratio. As shown in Figure 9, UBHC emission level decreased with the increasing biodiesel percentage.

The decreased trend of UBHC emissions of fuel might be presence of oxygen molecules in biodiesel helped for complete combustion. Figure 9 also gives UBHC emission results for different polanga biodiesel blends with injection pressures at full load. As seen in this figure, increased injection pressure decreased the UBHC emissions. The minimum UBHC emission (28 ppm) was obtained with B40 for 240 bar injection pressure. The increasing injection pressure caused the fuel air mixing in the combustion chamber was more excellent, so the UBHC emissions was obtained less than that of the high injection pressure. Lowest UBHC emission of 28 ppm was observed at 240 bar, which is 9 ppm lower than that of UBHC emission at 160 bar for the same biodiesel blend BD40. The reduction in UBHC emission of biodiesel is mainly due to the better vaporization and proper atomization. Further, the increasing of injection pressure improved the spray characteristics which led to better combustion.

#### 4.3.3 Oxides of nitrogen emissions

This is the most important emission attribute of biodiesel and its blends. NO<sub>x</sub> is the most dangerous gaseous emissions from engines; the reduction of it is always the goal for engine researchers and engine manufacturers. Thermal NO<sub>x</sub> refers to NO<sub>x</sub> formed through high temperature oxidation of nitrogen (N<sub>2</sub>) in combustion chamber. The formation of NO<sub>x</sub> highly

depends on in-cylinder temperatures, oxygen concentration and residence time for the reaction to take place, oxygen content of biodiesel is an central factor in the high NO<sub>x</sub> formation, because oxygen content of biodiesel provides high local peak temperatures and a equivalent excess of air. Figure 10 presents NO<sub>x</sub> emission values for different biodiesel blended diesel fuels and injection pressures at constant full load.

As observed increased injection pressure boosted the NO<sub>x</sub> emissions. Maximum NO<sub>x</sub> emissions was measured to be 807.37 ppm vol, 814.98 ppm vol, 846.1 ppm vol, and 898.05 ppm vol for BD10, BD20, BD30 and BD40 at 220 bar injection pressure, respectively. Increasing the injection pressure decreased the particle diameter and caused the biodiesel diesel fuel spray to vaporize quickly. However, the liquid fuel cannot penetrate deeply into the combustion chamber. So, higher injection pressure initially generates faster combustion rates, resulting in higher temperatures as shown in fig. As a consequence, NO<sub>x</sub> concentrations start to increase. The NO<sub>x</sub> emission level increases continuous with increasing injection pressure; this was because of faster combustion and higher cylinder gas temperature. Maximum NO<sub>x</sub> emission is 898.05 ppm vol at 240 bar of BD 40.

#### 4.3.4 Smoke opacity

Smoke formation occurs at extreme air deficiency. Air or oxygen deficiency is locally present inside the diesel engine. Table 3 shows smoke opacity results for different biodiesel-blended diesel fuels and injection pressures at constant load. It increases as the air–fuel ratio decreases. The smoke opacity increased with the increase of the engine load. The formation of smoke stoutly depends on the engine load. As the load increases, more fuel is injected, and this increases smoke formation. The results obtained in this study support this statement. At the ORG injection pressure, while smoke

opacity was measured to be 94% with B40 at full load. As illustrated in Figure 10 the smoke opacity decreased with the increase biodiesel percentage. The reduction of smoke opacity with increase of biodiesel in the fuel blend can be attributed to the decrease in the carbon content, and the increase of oxygen content, in the blended fuel. There is less C-C bond in the blended fuel with compared with more blending, resulting in the decrease of smoke opacity. At the same time, the oxygen in the fuel can assist in reducing smoke formation during the stage of diffusion combustion. When injection pressure is increased, fuel particle diameters will become smaller. Because formation of mixing fuel to air becomes better through injection period, smoke opacity will be less. It is very clear from the graph that for increasing injection pressure, the smoke emissions were reduced since cylinder operating temperatures were

higher at high injection pressure. Because of higher temperature and pressure there is an improved reaction between fuel and oxygen, and thus reduces the smoke. Figure 11 depicts smoke opacity results for different polanga biodiesel blend fuels with injection pressures at constant full load.

BD40 shows the lowest smoke emissions for all the injection pressure 95.3%, 94%, 93.4%, 92.5% and 92% at 160, 180, 200, 220 and 240 bar injection pressure respectively, it may be due to oxygen molecule in the biodiesel, which helps to promote stable and complete combustion by delivering oxygen to the prolepsis zone of the burning fuel by reducing locally over rich region and limit primary smoke formation, results in lower smoke emissions. Reduction in smoke level of biodiesel is due to its oxygen content and small particle diameter of injected fuel with high injection pressure.

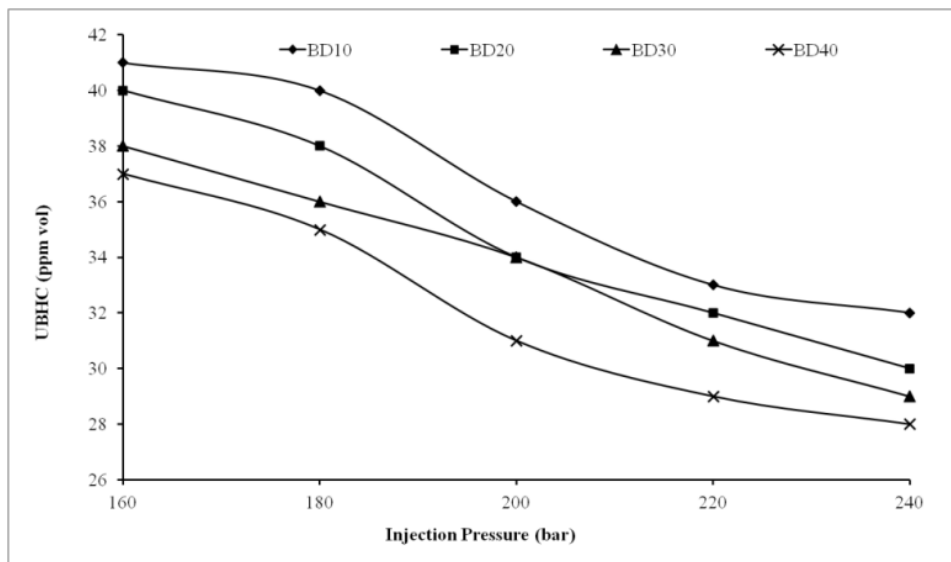


Fig. 9. Variation of UBHC at full load with injection pressure.

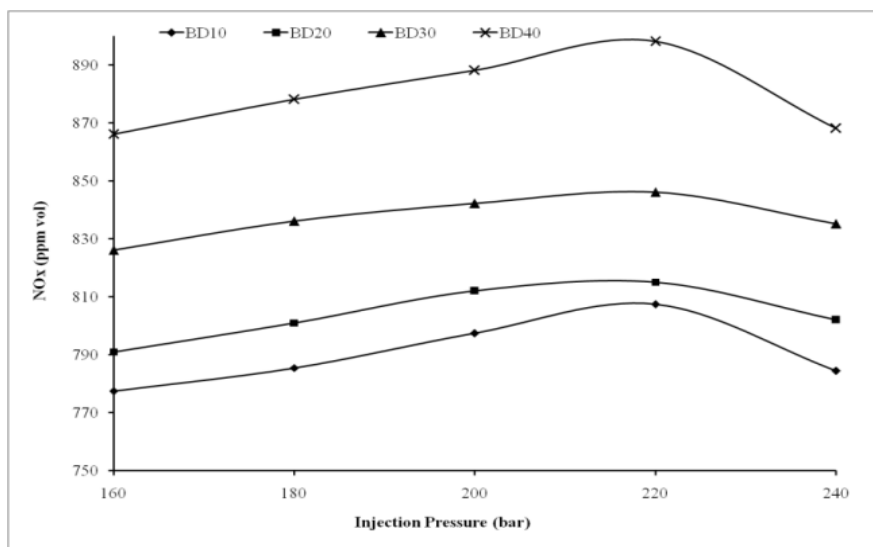


Fig. 10. Variation of NOx with injection pressure.

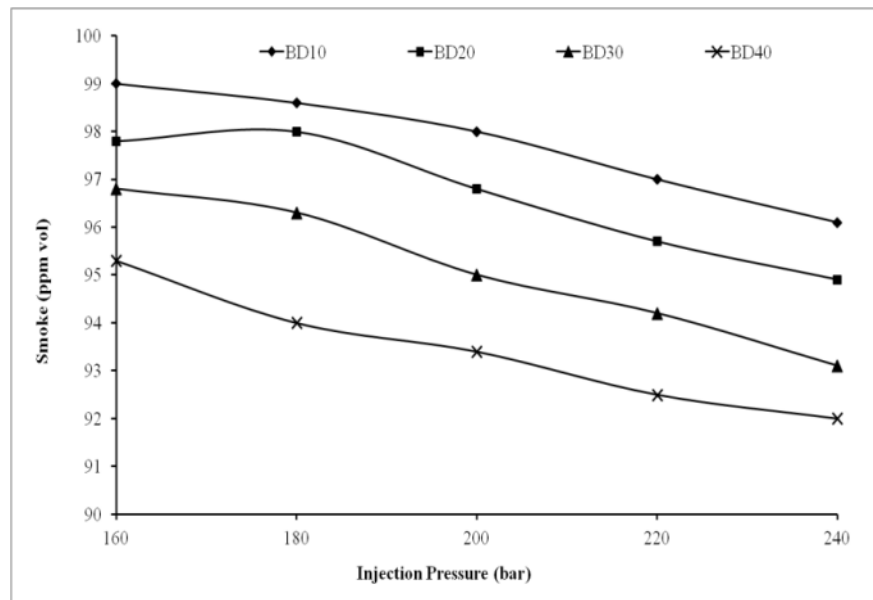


Fig. 11. Variation of smoke emission with injection pressure.

**4.4 Prediction of engine performance and exhaust emissions using ANN**

ANN model is considered as a sensible and reliable approach for non-linear problems. The input parameters of the network are blends of Polanga with diesel at different injection pressures and performance parameters brake specific fuel consumption (BSFC), brake thermal efficiency(BTE), exhaust gas temperature (Tex), carbon monoxide (CO), oxide of nitrogen (NOx), smoke and UBHC emissions are taken as output parameters. In this study, a computer program has been developed in MATLAB 2010a platform to predict brake specific fuel consumption (BSFC), brake thermal efficiency(BTE), exhaust gas temperature (Tex), carbon monoxide (CO), oxide of nitrogen (NOx), smoke and UBHC emissions of the engine. The most favorable network structures and statistical parameters of ANN models for diverse learning algorithms are given in Table 4. It was evident from Table 4, the prediction performances for both training and testing sets of performance and emission showed that all the approaches provided a fairly acceptable accuracy. Their R values were more than 0.99. The most excellent forecast results were obtained by LM learning algorithm. The LM learning algorithm had the premier speed compared with the other learning algorithms and it reached to best possible solutions with lesser number of neurons in hidden layer. Comparisons of the ANN predictions and trial results for testing sets of output performance and exhaust emissions parameters are verified in Figures 12a and 12b. The most outstanding point here is that the prediction results are extremely close to the trial results

As shown in Figure 12, the predictive capability of the network for performance and exhaust emissions parameters was found to be acceptable. This means that the choice of two input parameters as influencing dynamics for predictions of engine performance and exhaust emissions provides reasonable results. The

equations of the brake specific fuel consumption (BSFC), brake thermal efficiency (BTE), exhaust gas temperature (Tex), carbon monoxide (CO), oxide of nitrogen (NOx), smoke and UBHC emissions are given in Equations (3) to (9).

$$BSFC = \frac{1}{1 + e^{-(\sum_{i=1}^3 w_{2i} F_i + 0.34313)}} \tag{3}$$

$$BTE = \frac{1}{1 + e^{-(\sum_{i=1}^3 w_{2i} F_i + 27.144)}} \tag{4}$$

$$T_{ex} = \frac{1}{1 + e^{-(\sum_{i=1}^3 w_{2i} F_i + 0.35893)}} \tag{5}$$

$$CO = \frac{1}{1 + e^{-(\sum_{i=1}^3 w_{2i} F_i + 0.21331)}} \tag{6}$$

$$NOx = \frac{1}{1 + e^{-(\sum_{i=1}^3 w_{2i} F_i + 0.55572)}} \tag{7}$$

$$Smoke = \frac{1}{1 + e^{-(\sum_{i=1}^3 w_{2i} F_i - 5.2244)}} \tag{8}$$

$$UBHC = \frac{1}{1 + e^{-(\sum_{i=1}^3 w_{2i} F_i - 1.40738)}} \tag{9}$$

where  $F_i$  ( $i = 1, 2, 3, \dots, n$ ) can be calculated according to equation 2 in which  $NTi$  is the weighted sum of the inputs, and is calculated using

$$NTi = (w_{11} \times IP + w_{12} \times BD + b_i) \tag{10}$$



The data flow was completed with the weights Equations (3) to (9) are given in the Tables 6 and 7. The weight values appearing in

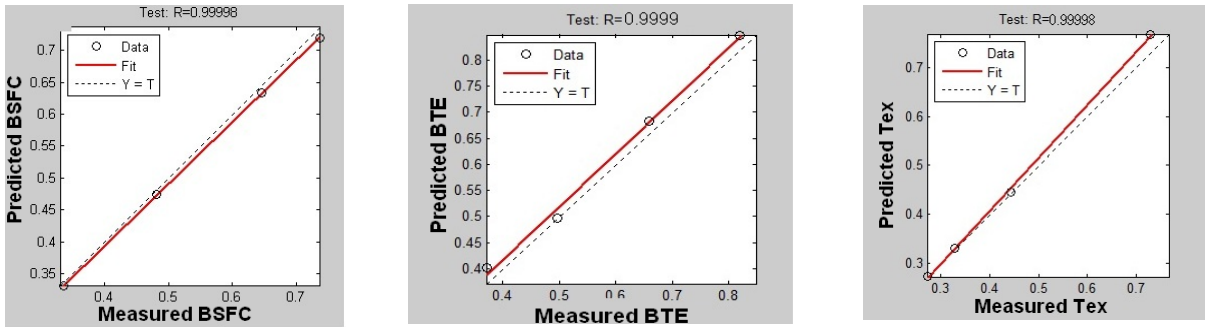


Fig. 12. (a) Predicted and experimental results for testing sets of performance parameters.

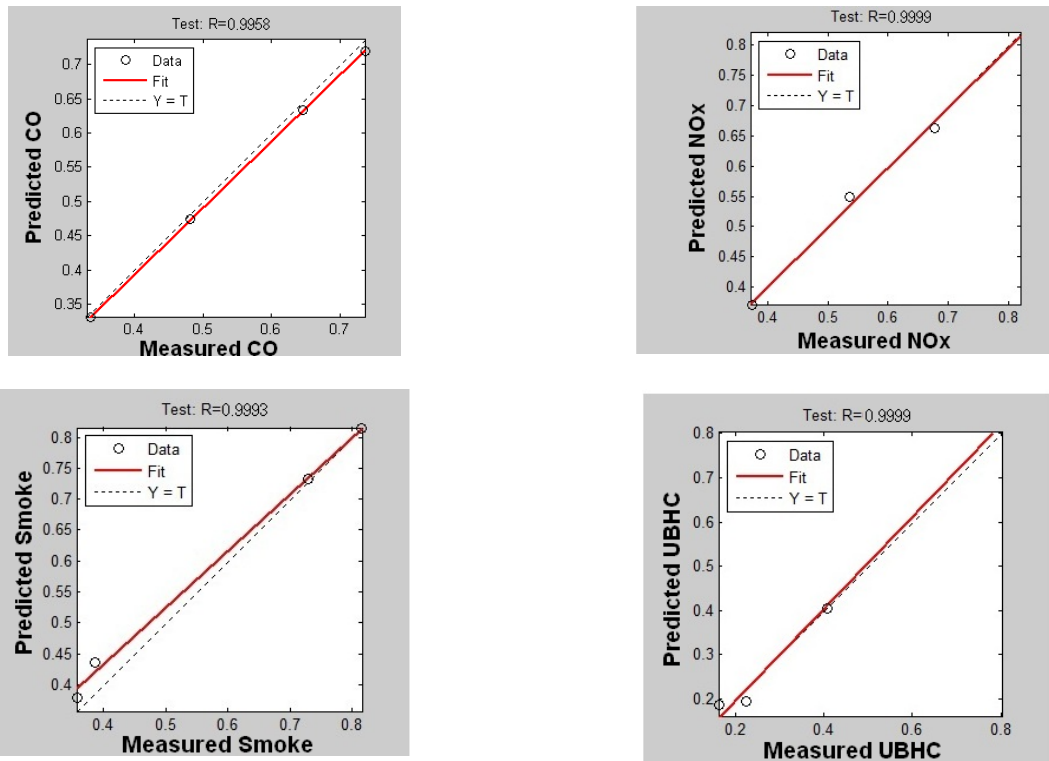


Fig. 12. (b) Predicted and experimental results for testing sets of emission parameters.

Table 6. Weights between input layer and hidden layer for performance parameters.

	<i>i</i>	$w_{11}$	$w_{12}$	$b_1$	$w_2$
BTE	1	-1.606	-0.33597	0.69548	-3.5387
	2	1.9041	0.17425	0.089628	-6.3514
	3	2.3992	-0.04936	0.75344	3.2473
BSFC	1	-8.4865	-2.1788	7.6867	-2.3812
	2	3.9897	-7.4609	-4.8474	-0.03029
	3	6.8536	-3.178	-4.753	-4.4348
	4	5.3832	-5.2183	-2.5869	2.4336
	5	-5.7181	-5.1586	-1.6053	0.60699
	6	-1.7805	-7.7431	-3.2877	-0.40463
	7	6.2135	-5.0013	4.6958	1.9296

	8	6.8669	-2.51	8.8412	1.8265
Tex	1	1.5451	-6.6139	-4.0683	-0.47135
	2	1.7902	1.8627	-2.3114	2.1142
	3	-6.7453	-0.53401	-1.2285	-1.9449
	4	-7.0123	0.59678	-0.16528	0.86299
	5	-5.9686	-1.4068	-3.2659	-0.26475
	6	5.3103	-2.0479	8.4219	-0.52849

Table 7. Weights between input layer and hidden layer for emission parameters.

	$i$	$w_{11}$	$w_{12}$	$b_1$	$w_2$
CO	1	-4.9444	-5.166	6.6262	-2.2294
	2	4.3453	3.5113	-1.2051	2.4863
	3	1.5648	6.6333	-0.5072	-0.2532
	4	2.744	-5.7003	2.3061	-0.1959
	5	3.8648	2.9246	3.0417	2.8129
	6	-6.641	-1.0035	-6.6432	-0.1159
NOx	1	-7.8727	0.39004	3.466	1.1739
	2	0.19278	-1.5302	0.62291	-2.1956
	3	5.2309	1.0656	3.7598	1.1605
	4	-0.82161	5.7447	3.1143	0.56433
Smoke	1	2.1236	1.567	-5.9787	-2.1376
	2	21.6831	-16.1722	-3.6952	-1.7645
	3	-1.129	0.7635	-0.3215	-3.2821
	4	-0.0311	-2.783	-11.776	0.06438
UBHC	1	-4.0605	6.5114	11.7625	1.0639
	2	-4.5533	0.14418	-1.355	1.0155
	3	-1.675	-1.5619	-0.1434	2.1475
	4	3.142	-6.8655	7.6305	-0.3846

Table 8. MPE and MSE for training and testing.

Output	MPE		MSE	
	training	test	training	test
BSFC	0.137	0.437	0.00465	0.0123
BTE	0.3423	0.00983	0.00435	0.0147
CO	1.22319	2.57923	0.00532	0.0169
NOx	0.1384	0.4032	0.00462	0.0118
Smoke	0.2028	0.1286	0.00447	0.0115

## 5. EVALUATION OF RESULTS

The network was trained successfully and then the test data was used to evaluate the selected network. Using results obtained from the network, a comparison was carried out using statistical methods. The performance of the network was evaluated using mean percentage error. Mean percentage error is the mean ratio between

the error and the experimental values. It indicates how large the error is related to the correct value and it is expressed in percentage values. The mean percentage errors and mean squared errors of the output parameters of optimum network for training and testing data are shown in Table 8.

Mean percentage errors were smaller than 2% and 3% for training and test data respectively. Hence, the

results obtained from optimum ANN model may easily be considered to be within the acceptable limits. Lower value of mean percentage error shows that there is a better correlation between trained or tested values and measured values.

## 6. CONCLUSION

The different polanga biodiesel blends in the present work can be conveniently used in 4 stroke single cylinder diesel engines as blends with diesel without any engine alterations. Experimental examination showed that the injection pressure of 240 bars was found to be the optimum condition for engine with BD40 biodiesel, based on the drop in BSFC and upgrading in brake thermal efficiency was also observed. Biodiesel blends resulted in the fall in CO, UBHC and smoke emission at elevated injection pressures. However NO<sub>x</sub> emission slightly increased with increasing injection pressures. Among the a range of injection pressure, 240 bars exhibited shorter ignition delay with slightly longer combustion. Multilayer feed forward network with back propagation training algorithm was used to predict the performance, emission and combustion features of diesel engine at various injection pressures. The predicted R values were found to be very close to unity while the MSE error was less than 0.0004 for BSFC, BTE, Tex, CO, NO<sub>x</sub>, smoke and UBHC and revealed that there was good correlation between the predicted and measured data. Analysis of the experimental data by the ANN revealed that there was good correlation between the predicted data resulted from the ANN and measured ones. The developed model thus reduces the experimental efforts and hence can serve as an effective tool for predicting the performance of the engine and emission characteristics under various operating conditions with different biodiesel blends.

## REFERENCES

- [1] Ghobadian B., Rahimi H., Nikbakht A.M., Najafi G., and Yusaf T.F., 2009. Diesel engine performance and exhaust emission analysis using waste cooking biodiesel fuel with an artificial neural network. *Renewable Energy* 34(4): 976–982.
- [2] Sahoo P.K., Das L.M., Babu M.K.G., and Naik S.N., 2007. Biodiesel development from high acid value polanga seed oil and performance evaluation in a CI engine. *Fuel* 86: 448–454.
- [3] Baiju B., Naik M.K., and Das L.M. 2009. A comparative evaluation of compression ignition engine characteristics using methyl and ethyl esters of Karanja oil. *Renewable Energy* 34:1616–1621.
- [4] Ramadhas A.S., Jayaraj S., and Muraleedharan C., 2005. Biodiesel production from high FFA rubber seed oil. *Fuel* 84:335–340.
- [5] Sahoo P.K., Das L.M., Babu M.K.G., Arora P., Singh V.P., Kumar N.R., and Varyani T.S., 2009. Comparative evaluation of performance and emission characteristics of jatropha, karanja and polanga based biodiesel as fuel in a tractor engine. *Fuel* 88: 1698–1707.
- [6] Shivakumar, Srinivasa P., Shrinivasa B.R., 2011. Artificial Neural Network based prediction of performance and emission characteristics of a variable compression ratio CI engine using WCO as a biodiesel at different injection timings. *Applied Energy* 88: 2344–2354.
- [7] Canakci M. and J.V. Gerpen. 2003. Comparison of engine performance and emissions for petroleum diesel fuel, yellow-grease biodiesel and soybean-oil biodiesel. *Transactions of the ASAE* 46(4): 937–944.
- [8] Canakci M., Ozsezen A.N., Arcaklioglu E., and Erdil A., 2009. Prediction of performance and exhaust emissions of a diesel engine fuelled with biodiesel produced from waste frying palm oil. *Expert Systems with Applications* 36: 9268–9280.
- [9] Yusaf T.F., Buttsworth D.R., Saleh K.H., Yousif B. F., 2010. CNG-diesel engine performance and exhaust emission analysis with the aid of artificial neural network. *Applied Energy* 87: 1661–1669.
- [10] Ismail H.M., Kiat N.H., Queck C.W., and Gan S., 2012. Artificial neural networks modelling of engine-out responses for a light-duty diesel engine fuelled with biodiesel blends. *Applied Energy* 92: 769–777.
- [11] Çay Y., Korkmaz I., Çiçek A., and Kara F., 2013. Prediction of engine performance and exhaust emissions for gasoline and methanol using artificial neural network. *Energy* 50: 177–186.
- [12] Wong K.I., Wong P.K., Cheung C.S., Vong C.M., 2013. Modeling and optimization of biodiesel engine performance using advanced machine learning methods. *Energy* 55: 519–528.
- [13] Javed S., Murthy Y.V.V.S., Baig R.U., and Rao D.P., 2015. Development of ANN model for prediction of performance and emission characteristics of hydrogen dual fueled diesel engine with Jatropha Methyl Ester biodiesel blends. *Journal of Natural Gas Science and Engineering* 26: 549–557.
- [14] Wong P.K., Wong K.I., Vong C.M., and Cheung C.S., 2015. Modeling and optimization of biodiesel engine performance using kernel-based extreme learning machine and cuckoo search. *Renewable Energy* 74:640–64.